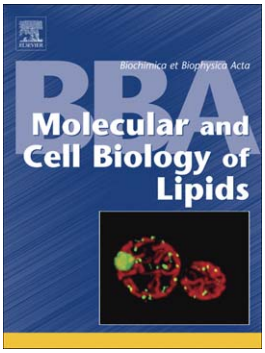

Cryptotanshinone promotes commitment to the brown adipocyte lineage and mitochondrial biogenesis in C3H10T1/2 mesenchymal stem cells via AMPK and p38-MAPK signaling

Khan Mohammad Imran, Naimur Rahman, Dahyeon Yoon, Miso Jeon, Byong-Taek Lee, Yong-Sik Kim

PII: S1388-1981(17)30148-8
DOI: doi:10.1016/j.bbalip.2017.08.001
Reference: BBAMCB 58190

To appear in: *BBA - Molecular and Cell Biology of Lipids*

Received date: 28 March 2017
Revised date: 7 August 2017
Accepted date: 9 August 2017

Please cite this article as: Khan Mohammad Imran, Naimur Rahman, Dahyeon Yoon, Miso Jeon, Byong-Taek Lee, Yong-Sik Kim, Cryptotanshinone promotes commitment to the brown adipocyte lineage and mitochondrial biogenesis in C3H10T1/2 mesenchymal stem cells via AMPK and p38-MAPK signaling, *BBA - Molecular and Cell Biology of Lipids* (2017), doi:10.1016/j.bbalip.2017.08.001

Cryptotanshinone promotes commitment to the brown adipocyte lineage and mitochondrial biogenesis in C3H10T1/2 mesenchymal stem cells via AMPK and p38-MAPK signaling

Khan Mohammad Imran[1,2,†], Naimur Rahman[1,2,†], Dahyeon Yoon[1,2], Miso Jeon[1,2], Byong-Taek Lee[2,3], and Yong-Sik Kim[1,2,*]

1. Dept. of Microbiology, College of Medicine, Soonchunhyang University

2. Institute of Tissue Regeneration, College of Medicine, Soonchunhyang University

3. Dept. of Tissue Engineering, College of Medicine, Soonchunhyang University

†: Equally contribution

* Corresponding author: Yong-Sik Kim, Ph.D.

Department of Microbiology, College of Medicine

Soonchunhyang University

Soonchunhyang 2gil 6, Dongnam-Gu, Cheonan, Chung-nam, 330-090, Korea

Tel: +82-41-570-2413

Fax: +82-41-575-2412

Email: yongsikkim@sch.ac.kr

Abstract

Although white adipose tissue (WAT) stores triglycerides and contributes to obesity, brown adipose tissue (BAT) dissipates energy as heat. Therefore, browning of WAT is regarded as an attractive way to counteract obesity. Our previous studies have revealed that treatment with cryptotanshinone (CT) during adipogenesis of 3T3-L1 cells inhibits their differentiation. Here, we found that pretreatment of C3H10T1/2 mesenchymal stem cells with CT before exposure to adipogenic hormonal stimuli promotes the commitment of these mesenchymal stem cells to the adipocyte lineage as confirmed by increased triglyceride accumulation. Furthermore, CT treatment induced the expression of early B-cell factor 2 (*Ebf2*) and bone morphogenetic protein 7 (*Bmp7*), which are known to drive differentiation of C3H10T1/2 mesenchymal stem cells toward preadipocytes and to the commitment to brown adipocytes. Consequently, CT treatment yielded brown-adipocyte-like features as evidenced by elevated expression of brown-fat signature genes including *Ucp1*, *Prdm16*, *Pgc-1α*, *Cidea*, *Zic1*, and beige-cell-specific genes such as *CD137*, *Hspb7*, *Cox2*, and *Tmem26*. Additionally, CT treatment induced mitochondrial biogenesis through upregulation of *Sirt1*, *Tfam*, *Nrf1*, and *Cox7a* and increased mitochondrial mass and DNA content. Our data also showed that cotreatment with CT and BMP4 was more effective at activating brown-adipocyte-specific genes. Mechanistic experiments revealed that treatment with CT activated AMPKα and p38-MAPK via their phosphorylation: the two major signaling pathways regulating energy metabolism. Thus, these findings suggest that CT is a candidate therapeutic agent against obesity working via activation of browning and mitochondrial biogenesis in C3H10T1/2 mesenchymal stem cells.

Keywords: C3H10T1/2, Cryptotanshinone, Browning, Ucp1, AMPKα, p38-MAPK

1. Introduction

In mammals, there are two distinct types of functionally and metabolically active adipose tissues, namely, white adipose tissue (WAT) and brown adipose tissue (BAT). WAT is specialized for the storage of chemical energy, in the form of large droplets of triglycerides, and expansion of WAT in both the number and size of cells leads to obesity. In contrast, BAT contains multiple small fat droplets and generates heat in response to cold exposure: a process called *nonshivering thermogenesis* [1]. The thermogenic capacity of brown fat cells is due to the possession of a large number of mitochondria and abundant expression of mitochondrial uncoupling protein 1 (UCP1) [2,3]. It is believed that an increase in the number of mitochondria or in mitochondrial biogenesis is a key feature of BAT and is regulated by several proteins encoded by nuclear and mitochondrial genomes, e.g., Tfam, nuclear transcription factor 1 (Nrf1), and cytochrome c oxidase subunits Cox7a and Cox8b [4]. It has been previously reported that BAT disappears after infancy, but recent evidence showed that metabolically active BAT is also present in adult humans [5,6]. Moreover, lately, brown-fat-like cells (also known as beige cells) were discovered in WAT [7]. A growing number of studies revealed that browning of WAT improves energy expenditure and reduces the risk of obesity-related metabolic syndrome [8–11]. Thus, stem cell commitment to brown or beige adipocytes, stimulation of BAT thermogenesis, and browning of WAT are regarded as possible approaches to treatment or prevention of obesity and its related metabolic complications [12].

Peroxisome proliferator-activated receptor (PPAR) γ coactivator 1α (PGC-1α), a transcriptional coactivator of UCP1, plays an important role by enhancing mitochondrial function and gene expression as well as by promoting the browning of WAT [4]. Moreover,

several transforming growth factor-β (TGF-β) targets such as bone morphogenetic proteins (BMP4 and BMP7) have been found to promote brown-fat-like characteristics in several cell types such as C3H10T1/2 and 3T3-L1 [13–17]. Some studies have indicated that BMP4 and BMP7 induce browning of human adipose stem cells and mouse C3H10T1/2 mesenchymal stem cells [16,17]. Moreover, recently, it was reported that several plant-derived hormones and anti-adipogenic natural compounds such as abscisic acid [18], curcumin [19], resveratrol [20], sulforaphane [21], and butein [22] induce a brown-fat-like phenotype in 3T3-L1 cells and primary white adipocytes.

A natural compound from the plant *Salvia miltiorrhiza* (danshen) called cryptotanshinone (CT) has been shown to exert several pharmacological effects such as antioxidant, anti-inflammatory, anticancer, antitumor, antiangiogenesis, and antidiabetic [23]. CT inhibits tumor growth in an *in vivo* model [24]. Although an *in vivo* study confirmed that CT treatment can reduce body fat, cholesterol, and triglyceride formation in mice, the underlying molecular mechanism is still unclear [23]. Moreover, in our previous study, we showed that CT inhibits 3T3-L1 preadipocyte differentiation through modulation of the STAT3 pathway during early adipogenesis [25].

Here, we studied the effect of CT on the browning (increasing brown fat cell-like characteristics) of C3H10T1/2 mesenchymal stem cells by causing them to commit to the adipocyte cell lineage with brown fat cell-like characteristics rather than white adipocytes or even the chondrocyte and myocyte cell lineages. We also compared the browning effect of CT with that of BMP4. We show that CT effectively upregulates the key BAT-related markers, mitochondrial-biogenesis-related markers, and several beige-cell-specific markers

while inhibiting the expression of WAT-specific markers through AMPKα, p38-MAPK, and Smad signaling in C3H10T1/2 cells.

2. Materials and methods

2.1. Materials

CT (purity ≥98%, HPLC), rosiglitazone, dexamethasone, isobutyl-1-methylxanthine (IBMX), insulin, 4′,6-diamidino-2-phenylindole (DAPI), Oil Red O dye (ORO), dorsomorphin (Dorso), SB203580, 4% formaldehyde, and dibutyryl adenosine 3′,5′-cyclic monophosphate (cAMP, purity ≥98%, HPLC) were purchased from Sigma-Aldrich (St. Louis, MO, USA). Dulbecco's modified Eagle's medium (DMEM), and recombinant human BMP4 were acquired from Gibco (Grand Island, NY, USA). Fetal bovine serum (FBS) was purchased from Atlas Biologicals (Fort Collins, CO, USA). A Penicillin-Streptomycin solution was purchased from Hyclone Laboratories, Inc. (South Logan, NY, USA). Mitotracker red probes, antibodies against phospho (p)-Smad1/5 (Ser 463/465), Smad1, p38, p-p38 (Thr180/Tyr182), p-AMPKα (Thr172), AMPKα, p-ERK1/2 (Thr202/Tyr204), ERK1/2, JNK2, p-SAPK/JNK (Thr183/Tyr185), Sirt1, and F(ab')2 Fragment (Alexa Fluor® 488 Conjugate) as well as horseradish peroxidase (HRP)-conjugated anti-rabbit IgG antibodies were purchased from Cell Signaling Technology (Danvers, MA, USA). Antibodies against Ucp1, Pgc1a, Prdm16, and β-actin were acquired from Abcam (Cambridge, MA, USA). The BCA Protein Assay Kit was purchased from Thermo Scientific (Rockford, IL, USA). Protein-loading buffer was acquired from Bio-Rad Laboratories, Inc. (Hercules, CA, USA). Bodipy 493/503 was purchased from Life Technologies Corporation (Carlsbad, CA, USA), and Dual-Luciferase® Reporter Assay System from Promega, Inc.

2.2. Cell culture, differentiation, and treatment

C3H10T1/2 mouse mesenchymal stem cells were obtained from Korean Cell Line Bank (KCLB-10226), and mouse iWAT cells were kindly provided by Yun-Hee Lee, Yonsei University. These cells were maintained in high-glucose DMEM, supplemented with 10% (v/v) of FBS, and 1% (v/v) of the antibiotic–antimycotic solution (100 U/mL penicillin, 100 U/mL streptomycin) in a humidified atmosphere containing 5% of CO_2 at 37°C (in a CO_2 incubator). To induce commitment, C3H10T1/2 cells were seeded at low density to obtain 20–30% confluence the following day. Next day, we started to incubate the cells with or without 50 ng/mL human recombinant BMP4 until the cells became completely confluent. The medium was replenished every 2 to 3 days. At 48 hr post-confluence, differentiation was induced by changing the medium to DMEM containing 10% of FBS, and MDI (0.5 mM IBMX, 1 μM Dexamethasone, and 10 μg/mL Insulin) in the presence or absence of 8 μM CT designated as day 0. Then, the media were replenished every other day with DMEM containing 10% of FBS and 10 μg/mL insulin with or without 8 μM CT until day 8. To stimulate the thermogenic program, the differentiated cells were exposed to 500 μM dibutyryl cAMP for 4 hr. Mouse iWAT cells were seeded at 40–50% confluence to attain full confluence on another day, when they were incubated with a growth medium containing 10 μg/mL insulin and 1 nM T3 (Triiodothyronine) with or without 8 μM CT. On the next day, the cells were incubated with a growth medium containing MDI with or without 8 μM CT. The medium was replenished every other day. 3T3-L1 mouse embryo fibroblast cells were obtained from Korean Cell Line Bank (KCLB-10092.1) and were maintained and differentiated as previously described [26].

2.3. Analysis of mitochondrial content by immunofluorescent staining and quantitative real-time PCR (qRT-PCR)

C3H10T1/2 cells were plated onto glass coverslips in 35-mm dishes. After 10 days of differentiation, cell monolayers were washed twice with 1× phosphate buffered saline (PBS) and incubated with the Mitotracker stain (diluted in a growth medium at a concentration of 100 nM) for 15 min at 37°C. After that, the cells were fixed in ice-cold methanol for 15 min at −20°C, then rinsed three times with PBS for 5 min each. Next, the cells were permeabilized with 0.1% Triton X-100 in 3% BSA for 15 min and blocked with 1% BSA, 5% goat serum, and 0.3% Triton X-100 in 1× PBS for 1 hr at room temperature. The cells were then incubated overnight at 4°C with a primary antibody against Ucp1 (Abcam), then with an Alexa Fluor 488-conjugated anti-rabbit IgG (secondary) antibody (Cell Signaling Technology) for 1 hr at room temperature. For DNA staining, the cells were incubated with 1 μg/mL DAPI for 1 min at room temperature, then washed three times with 1× PBST (PBS, 0.25% Tween 20). Coverslips were mounted with a fluorescent mounting medium containing an anti-fading agent (Dako, CA, USA). Images were captured using a confocal microscope (Olympus; Tokyo, Japan) and analyzed in the FV10i-ASW 3.0 Viewer software. The images were processed as described elsewhere [27]. Briefly, immunostaining images were converted to weighted 8-bit grayscale images, then inverted, and signals were quantified by densitometry in ImageJ (http://rsb.info.nih.gov/ij).

Mitochondrial biogenesis was quantified assuming that nuclear DNA (nDNA) remains constant but the ratio of the amounts of mitochondrial DNA (mtDNA) to nDNA increases. mtDNA and nDNA were quantified by real-time qPCR as previously described [28]. For each DNA extract, ribosomal protein large p0 (nuclear gene) and the mitochondrial gene

cytochrome c oxidase subunit I (CoxI) were quantified individually by qRT-PCR. Data were normalized to the nuclear gene *p0* DNA (ΔΔCT analysis).

2.4. Bodipy 493/503 lipid staining

C3H10T1/2 cells were grown on glass coverslips in 35-mm dishes and differentiated for 10 days. The Bodipy green stain was diluted with 1× PBS (to 1 μM) and incubated with the fixed cells for 15 min, then the cells were washed three times with 1× PBS and incubated with 1 μg/mL DAPI for 1 min at room temperature, and washed three times with 1× PBS. Images were captured using a confocal microscope (Olympus; Tokyo, Japan) with an Alexa Fluor® 488 dye excitation and emission wavelength and analyzed FV10i-ASW 3.0 Viewer software (Olympus; Tokyo, Japan).

2.5. qRT-PCR analysis

Total RNA was extracted using an RNA Extraction Kit (Qiagen, Valencia, CA, USA), according to the manufacturer's instructions, and the concentration was measured using scandrop spectrophotometer Analytik Jena AG (Jena, Germany). A total of 1 μg of RNA was subjected to reverse-transcriptase PCR to synthesize cDNA with the Maxime RT PreMix kit (Intron Biotechnology, Seoul, Korea), and the reaction was run on a Veriti 96-Well Thermal Cycler (Applied Biosystems, Singapore). qRT-PCR was conducted using an iQ™ SYBR Green Supermix kit (Bio-Rad, Singapore) on a CFX96™ Real Time PCR detection system (Bio-Rad, Singapore). The sequences of the primers are listed in Table 1. The magnitude of expression was normalized to that of *Gapdh*.

2.6. Preparation of whole-cell extracts and western blot analysis

Prior to harvesting, untreated and treated cells were washed twice with ice-cold 1× PBS and lysed in RIPA lysis buffer supplemented with a protease inhibitor cocktail, 2 mM PMSF, 1 mM sodium orthovanadate (Santa Cruz, CA, USA), and a phosphatase inhibitor cocktail (Sigma-Aldrich St. Louis, MO, USA). The lysates were harvested by scraping, incubated on ice for 15 min, and centrifuged at 14,000 × *g* for 15 min at 4°C to collect the supernatant. Protein concentration was determined using the BCA Protein Assay Kit. Equal amounts of protein were loaded for each sample and separated on a 4–20% sodium dodecyl sulfate polyacrylamide gradient gel (Mini-PROTEAN Precast Gel, Bio-Rad). After electrophoretic separation, the proteins were transferred onto a polyvinylidene difluoride (PVDF) membrane (Trans-Blot SD Semi-Dry Cell, Bio-Rad) using a semidry transfer cell (Bio-Rad) at 13 V for ~1.5 hr. The membranes were then blocked with 5% dried skim milk in 1× Tris-buffered saline (TBS) containing 0.1% Tween 20 for 1 hr at room temperature on a shaker, and next incubated with primary antibodies overnight at 4°C. After that, the membranes were washed three times for ~5 min at room temperature. The PVDF membrane was then incubated with agitation on a shaker with a specific horseradish peroxidase-conjugated secondary antibody for 1.5 hr at room temperature followed by three washes for ~5 min each. All washing steps were performed in 1× TBS containing 0.1% Tween 20. Immunoreactive protein signals were detected using the chemiluminescent ECL assay, and images were acquired by means of molecular image software ImageLab 2.0 (Bio-Rad), then processed by densitometry in the ImageJ software. Minor adjustment of brightness and contrast was carried out for better visualization of data, but the same changes were applied to the complete image panel as a

whole, and no information was lost from the image. An anti-β-actin antibody served as the loading control for each protein's expression.

2.7. A reporter assay

C3H10T1/2 and 3T3-L1 cells were seeded at 70–80% confluence in 48-well plates and transfected with 1.0 μg of the pGL3/3.1kb Ucp1-Luc reporter (Kindly provided by Prof. Leslie P. Kozak, Institute of Animal Reproduction and Food Research, Polish Academy of Sciences, Olsztyn, Poland) and 20 ng of *Renilla* Luciferase-expressing vectors by means of Lipofectamine 2000 (Invitrogen, Carlsbad, CA) by following the manufacturer's protocol. At 24 hr after the transfection, the cells were treated as mentioned above then collected and assayed after 24 hr (of treatment) by means of the Dual-Luciferase Reporter Assay System (Promega) following the manufacturer's protocol.

2.8. p38-MAPKα gene silencing study

Low passage number C3H10T1/2 MSCs were transfected with a p38-MAPKα siRNA (Santa Cruz Biotechnology, Inc.) at 80% to 90% confluence with Lipofectamine 2000 by following the manufacturer's protocol. Briefly, 100 pM siRNA was transfected with 6 μL/well Lipofectamine 2000 in 6-well plates. siRNA and Lipofectamine 2000 were separately diluted in 150 μL of the Opti-MEM medium (incubated for 5 min), mixed and then incubated for another 30 min at room temperature, and then added into designated well and mixed. The medium was removed and replaced with the induction medium (MDI) after 2 days of post-confluence in the presence or absence of CT. The efficiency of siRNA silencing was

determined by WB after 24 hr of transfection using p38 antibody. RNA was collected on day 2 of cell differentiation and subjected to qRT-PCR for the analysis of downstream genes.

2.9 Statistical Analyses

All data in this experiment are expressed as mean ± standard deviation (SD) of no less than three separate experiments. Unless otherwise stated MDI treated sample group was used as control to measure fold change. Significant differences between different treatment groups with control group (MDI) were calculated using Student's t-test. *P ≤ 0.05, **P ≤ 0.01, ***P ≤ 0.001. A P value of < 0.05 was considered statistically significant.

3. Results

3.1. CT promotes commitment of C3H10T1/2 mesenchymal stem cells to the adipocyte lineage but inhibits white adipogenesis in 3T3-L1 cells

To determine the effect of CT on lineage development of C3H10T1/2 mesenchymal stem cells, we added CT and BMP4 to the culture medium on day −3 of differentiation of C3H10T1/2 mesenchymal stem cells (Fig. 1A). Of note, after 8 day differentiation, differentiated adipocytes were observed in the CT treatment group (Fig. 1B). Next, we compared the effect of CT with that of a known inducer of C3H10T1/2 stem cell commitment, BMP4, and our data showed that CT treatment markedly induced lipid accumulation as compared with MDI treatment but not as much as BMP4 (Fig. 1B). In line with our previous study [25], we found that co-treatment with CT and adipogenic hormonal stimuli (MDI) inhibited the differentiation of 3T3-L1 preadipocytes (Fig. 1C). However, co-treatment with CT during MDI-stimulated commitment of C3H10T1/2 mesenchymal stem

cells caused a large number of C3H10T1/2 mesenchymal stem cells to commit to the adipocyte lineage as evidenced by increased triglyceride accumulation measured by ORO staining (Fig. 1C).

3.2. CT increases the expression of BAT-specific and beige-cell-specific genes but downregulates WAT-specific genes in C3H10T1/2 mesenchymal stem cells

To evaluate the ability of CT to induce brown-fat-like features in C3H10T1/2 adipocytes and to compare the browning effect of CT with that of BMP4 (because BMP4 is known to induce BAT-specific markers in white adipocytes [16]), we divided the cells into several treatment groups: MDI stimulation and supplementation of MDI-stimulated cells with CT or BMP4 or in combination (Fig. 2). Consistent with recent studies, pretreatment of cells with BMP4 before exposure to MDI resulted in elevation of mRNA levels of key BAT-specific markers *Ucp1*, *Pgc-1α*, *Prdm16*, deiodinase 2 (*Dio2*), *Cidea*, *PPARα*, epithelial V-like antigen 1 (*Eva1*), and *Zic1* as compared to cells treated only with MDI (control) (Fig. 2A). We also found that CT treatment markedly induced the mRNA level of *Pgc-1α* (~4-fold) and cotreatment with CT and BMP4 induced the mRNA level of *Pgc-1α* (8-fold). In agreement with these results, Prdm16 (an important early regulator of brown cell adipogenesis) was also significantly induced by CT treatment in presence or absence of BMP4 (Fig. 2A). Notably, the key brown fat thermogenic marker, *Ucp1*, was also upregulated by CT, whereas co-treatment with CT and BMP4 resulted in significant induction (Fig. 2A). Additionally, we observed an increase in the mRNA level of some other important brown-fat-specific genes, such as *Dio2*, *Cidea*, *Pparα*, *Eva1*, and *Zic1* under the influence of CT treatment in the

presence or absence of BMP4 (Fig. 2A). Because CT induces the key brown-fat-specific markers *Ucp1* and *Pgc-1α*, we next evaluated the effect of CT on beige-adipocyte markers (Fig. 2A). CT treatment induced major beige-cell-specific genes *Cd137*, *Hspb7*, *Cox2*, and *Tmem26*, whereas other beige-cell markers including *Tbx1*, *Fgf21*, and Arginase 1 were not induced [29]. Combined treatment with CT and BMP4 elevated the expression of *Cd137*, *Hspb7*, and *Tmem26* as compared with CT-only or BMP4-only treatment although *Cox2* expression was induced by CT and CT with BMP4 but not by BMP4 alone (Fig. 2A). On the other hand, CT treatment significantly reduced the mRNA level of key WAT-specific genes, *Psat1* and Resistin, while the expression of Serpina3k was not changed significantly (Fig. 2B). To understand the role of CT during adipocyte lineage development, we measured the expression of other lineage markers. As expected, CT treatment significantly inhibited the expression of other lineage markers (Fig. 2C). The expression of the key myogenesis critical marker *MyoG* was greatly reduced by CT co-treatment with BMP4. In addition, expression of chondrogenesis markers *Sox9*, *Col1a1*, and *Col2a1* was significantly reduced by CT treatment (Fig. 2C). These data suggested that CT may contribute to the adipogenic lineage development of MDI-induced C3H10T1/2 cells rather than to terminal differentiation.

3.3. CT promotes differentiation into brown adipocytes

Next, we tested whether CT can cause C3H10T1/2 mesenchymal stem cells to differentiate into brown adipocytes. First, we determined whether CT can induce expression of the brown-adipocyte marker Ucp1. Treatment of both C3H10T1/2 and 3T3-L1 cells with CT after transfection of a Ucp1-luc reporter showed that CT can dose-dependently induce the Ucp1 reporter activity as much as Forskolin (which is a known strong inducer [30]) (Fig. 3A). We

also measured the Ucp1, Prdm16, and Pgc-1α expression as compared with treatment with rosiglitazone: a PPARγ agonist and a well-known brown-adipocyte inducer (Fig. 3B). As shown in Fig. 3B, Ucp1 expression was enhanced threefold by rosiglitazone or CT treatment in C3H10T1/2 cells. The expression of Prdm16 was increased twofold and threefold by rosiglitazone and CT treatment, respectively. Pgc-1α expression was increased fourfold and threefold by rosiglitazone and CT treatment, respectively. We also observed a morphological change of C3H10T1/2 cells after the treatment with CT. According to Fig. 3C, C3H10T1/2 cells contained small, multilocular lipid droplets and a central nucleus in rosiglitazone or CT treatment group, whereas MDI-treated cells showed big, unilocular lipid droplet and a peripheral nucleus. These data suggest that CT treatment promotes thermogenic characteristics in C3H10T1/2 cells just like in brown adipocytes.

3.4. CT promotes mitochondrial biogenesis

Mitochondrial biogenesis and function are crucial for the thermogenesis of brown fat. Whereas CT induces the browning of C3H10T1/2 white adipocytes (stimulated by MDI) in both BMP4-dependent and -independent manner, next, we evaluated the effect of CT on mitochondrial mass and on the expression of mitochondrial biogenesis-related genes. In line with the above findings, nuclear respiratory factor 1 (Nrf1), mitochondrial transcription factor A (Tfam), and cytochrome oxidase subunit VIII a (Cox7a) were significantly upregulated by CT treatment in BMP4-pretreated cells, cytochrome c oxidase subunit VIII b (Cox8b) expression remained unchanged (Fig. 4A).We found that CT treatment markedly increased the expression of Pgc-1α (Fig. 3B), the key regulator of mitochondrial biogenesis [31,32] and

function in both BMP4-pretreated and untreated differentiating C3H10T1/2 cells. We next performed immunostaining with a Mitotracker- and Ucp1-specific antibody. As shown in Fig. 4B, in rosiglitazone- and CT-treated cells, mitochondrial content increased by 50% and 70% as compared with the MDI group. We also compared the effect of CT on mitochondrial biogenesis with that of a known inducer, rosiglitazone [33] (Fig. 4B). In addition, CT-treated cells showed a threefold increase in the expression of mitochondrial membrane protein Ucp1. Moreover, mitochondrial DNA content indicator, Cox1 expression, was increased twofold (Fig. 4B). Sirt1 is a marker of mitochondrial biogenesis [34]. As shown in Fig. 4C, Sirt1 expression was significantly increased by CT treatment of C3H10T1/2 cells. These data suggested that CT treatment also promotes mitochondrial biogenesis which strengthen the CT mediated brown adipogenesis findings.

3.5. CT specifically activates the p38-MAPK/AMPKα/Smad1/5 signaling in C3H10T1/2 cells

To understand the molecular mechanism of the commitment to the adipocyte lineage, first, we measured mRNA expression of early commitment markers including *Ebf2, Bmp7* and *Irf4*, which are known to be inducers of commitment of C3H10T1/2 mesenchymal stem cells to brown-fat preadipocytes [35,36]. While *Ebf2, Bmp7* and *Irf4* were induced but other bone morphogenetic genes such as *Bmp2*, *Bmp4*, and *Bmp5* were unaffected (Fig. 5A). Moreover, the expression of early B-cell factors 1 and 3 (*Ebf1* and *Ebf3*) was reduced (Fig. 5A). Previous study showed, Ebf1 promotes adipogenesis when overexpressed in NIH 3T3 fibroblasts, but Ebf3 is not required for adipogenesis [37]. As shown in Fig. 5B, CT-mediated activation of p38-MAPKα starts at 10 min and retained the activation until 60 min. Furthermore, CT activates AMPKα, the major regulator of energy metabolism by

phosphorylation and this activation is robust at 60 min (Fig. 5B). Of note, CT activates AMPKα by phosphorylation and reverses AMPKα phosphorylation from its specific inhibition by dorsomorphin (Fig. 5C). CT also phosphorylates p38-MAPK and reverses the SB203580 mediated inhibition of p38-MAPK (Fig. 5C). Dorsomorphin and SB203580 are well characterized specific inhibitor of AMPK and p38-MAPK, respectively [38,39]. Additionally, CT activates Smad signaling by phosphorylation of Smad1/5, a mediator of BMP signaling (Fig. 5C). We also investigate whether p38-MAPK and AMPK signaling contribute to the expression of brown adipocyte commitment-related genes, Bmp7, Ebf2, Prdm16, and Pgc-1α in CT-induced C3H10T1/2 mesenchymal stem cells. As shown in Fig. 5D, expression of genes of brown-adipocyte commitment—and markers of brown fat and mitochondrial biogenesis—was inhibited by the inhibition of AMPK and p38-MAPK but was ameliorated by CT treatment (Fig. 5D). In addition, a combinatory inhibition of AMPK and p38-MAPK showed more potent effect on the inhibition of those above mentioned commitment markers (Fig. 5D). Data suggest that CT governs the regulation of brown-adipocyte commitment by regulation of both p38-MAPK and AMPKα signaling.

To avoid unexpected inhibition by high dose SB203580, we conducted the experiment using gene silencing of p38-MAPKα. As shown in Fig. 6A, successful silencing of p38-MAPK gene showed inhibitory effect on AMPKα phosphorylation and Sma1/5 phosphorylation. Of note, silencing of p38-MAPKα gene also inhibited CT mediated induction of brown-adipocyte commitment markers expression (Fig. 6B). Taken together chemical inhibition and siRNA gene silencing data, we can propose that p38-MAPK is working upstream of AMPK and Smad1/5 and AMPK is working upstream of Smad1/5.

4. Discussion

Recently, a series of studies revealed that adult humans have a significant amount of metabolically active brown adipocytes with the ability to disperse energy in the form of thermogenesis [7,40,41]. Emerging evidence shows that an increased volume of BAT is associated with weight loss and energy consumption in obese subjects [42,43]. Thus, exploration of the factors that can induce BAT-like features in WAT may lead to a novel therapeutic strategy against obesity and related metabolic complications.

In the present study, we evaluated the effect of CT, a plant-derived quinoid diterpene on commitment of C3H10T1/2 pluripotent stem cells to the adipocyte lineage and possible formation of brown-fat-like characteristics in C3H10T1/2 and inguinal white adipose cells. We also tried to identify the underlying molecular mechanisms. In addition, we compared the effect of CT with that of BMP4 or rosiglitazone as a positive control of browning of white adipocytes [16,44].

CT treatment of C3H10T1/2 mesenchymal stem cells was found to promote the commitment of these cells to the adipocyte lineage rather than myocyte or chondrocyte lineages. This finding made us curious whether CT treatment drives these committed cells toward the brown- or beige-adipocyte cell lineage. It has been reported that a loss of Ebf2 in brown preadipose cells results in the decreased expression of brown preadipose-signature genes, whereas ectopic Ebf2 expression in myoblasts upregulates brown-preadipose-cell-specific genes [36,45]. Some data suggested that Ebf2 acts at the precursor cell stage to maintain the preadipose cell fate. Particularly, Ebf1 promotes adipogenesis when overexpressed in NIH 3T3 fibroblasts [36,37]. It has also been reported that Bmp signaling, in particular Bmp7, activate Ebf2, which is necessary for early BAT development and recruitment of beige

adipocytes [46]. A browning inducer, Bmp7, has been implicated in browning and mitochondrial biogenesis via regulation of AMPK phosphorylation [47]. Activation of the AMPK-mediated pathway is crucial for maintaining energy homeostasis [48]. One report revealed that only activation of AMPK takes place, but the total AMPK amount remains constant during the progression of browning [20]. Irisin induces browning of white adipocytes via p38-MAPK and ERK MAP kinase signaling [49]. Some researchers also demonstrated that Bmp signaling is crucial for the early commitment to the adipocyte lineage rather than adipocyte differentiation in C3H10T1/2 pluripotent stem cells via Smad and p38-MAPK signaling [50]. Furthermore, Smad signaling performs a crucial function in brown adipogenesis [13,51].

Our data showed that CT treatment activates AMPKα, p38-MAPK, and Smad1/5 by phosphorylation and significantly increases *Bmp7* transcription in comparison with other Bmp family members such as *Bmp2*, *Bmp4*, and *Bmp5*. Additionally, CT treatment of C3H10T1/2 cells leads to upregulation of *Ebf2*, whereas *Ebf1* and *Ebf3* expression levels were found to be significantly reduced. Moreover, CT activates both AMPKα and p38-MAPK and restores their activation during pharmacological inhibition. Pharmacological inhibition of AMPK and p38-MAPK reduces the expression of commitment and brown fat markers including *Ebf2* and *Bmp7*, but CT effectively reverses these effects, indicating that AMPK and p38-MAPK are both necessary for the browning process under the influence of CT. These data allow us to suggest that induction of Ebf2 and Bmp7 by the treatment with CT at the early stage of C3H10T1/2 cell differentiation may promote early commitment to the brown adipocyte lineage.

Previously, our group demonstrated that CT inhibits differentiation via regulation of C/EBPβ, and PPARγ, through activation of STAT3 in 3T3-L1 preadipocytes [25]. A recent paper has shown that BMP4-mediated browning of C3H10T1/2 cells is governed by the elevated expression of Ucp1 [17]. Furthermore, CT treatment dramatically up regulated Ucp1 reporter activity in C3H10T1/2 cells. In accordance with another study, CT treatment significantly increases the expression of Prdm16 and Pgc-1α and subsequently activates the expression of Ucp1. Expression of Prdm16 in white fat cells induces a complete program of brown-fat differentiation and mitochondrial-biogenesis-related genes [15,52,53]; these data correlate with our findings of induced brown-fat-, beige-cell-, and mitochondrial-biogenesis-related markers by CT treatment. Our data also suggest that CT treatment significantly increases the mRNA level of *Pparα*, which is highly expressed in white adipocytes treated with a β_3-adrenergic agonist, thus showing features of brown-fat-like adipocytes [54].

The thermogenic properties of BAT are governed by the activity of Ucp1 [2]. A lack of Ucp1 increases susceptibility to diet-induced obesity and abrogates diet-induced thermogenesis in mice [55,56]. In terms of Ucp1 transcriptional regulation, transcription factors PPARγ and Prdm16 and transcriptional coactivator Pgc-1α are key regulators [57,58]. Recently, some investigators found that forskolin, thiazolidinedione, retinoids, and isoproterenol regulate human Ucp1 transcription in an enhancer 3.5 kb upstream of the gene [30,59]. Reports also suggest that a 200-bp enhancer is positioned ~2.5 kb upstream of the transcription start site and contains (PPRE [60], TRE/RARE [61,62] and cAMP-responsive elements) cis-acting elements, which are intimately involved in the regulation of Ucp1 [63,64]. Of note, CT can effectively activate −3.1-kb Ucp1 promoter reporter activity in C3H10T1/2 cells. These results suggest that CT or its metabolites may activate Ucp1 via

regulation and recruitment of PPARγ, Prdm16, and Pgc-1α and induces brown adipogenesis of C3H10T1/2 cells although the mechanism of CT-mediated Ucp1 transcriptional regulation is not clear yet and needs further research.

Mitochondrial dysfunction in tissues has been proven to be a major factor in various diseases including diabetes and cancer [65–68]. The differentiation and physiological function of brown adipocytes are associated with enhanced mitochondrial biogenesis. The transcriptional coactivator Pgc-1α is the master regulator of mitochondrial activity and function [69]. Pgc-1α and Sirt1 regulate mitochondrial biogenesis and activate several genes such as *Nrf1*, which regulates the expression of Tfam [70–72]. In a fine review, de Oliveira et al. stated that resveratrol elicits mitochondrial biogenesis via multiple mechanisms, which mostly involve activation of Sirt1, Pgc-1α, Nrf1, Tfam, and AMPK pathways to increase mitochondrial number and mass [73]. Our data revealed that CT effectively induces mitochondrial-biogenesis-related genes: *Sirt1*, *Pgc1a*, *Nrf1*, *Cox7a*, and *Tfam*. We also observed a 70% increase in the mitochondria amount and mtDNA amount. These data suggest that CT may also contribute to mitochondrial homeostasis and biogenesis via a pathway similar to that of resveratrol; these phenomena need further investigation.

Our data revealed that *CD137*, *Hspb7*, *Cox2*, and *Tmem26* were also upregulated by CT treatment while *Tbx1*, *Fgf21*, and Arginase1 were not induced, indicating that CT induces the beige-adipocyte features in C3H10T1/2 cells only partially. Moreover, CT decreased the expression of resistin and Psat1; those are particularly highly expressed in white adipose tissue, while another white-adipose-tissue marker Serpina3k was barely affected by CT treatment. These data suggest that CT effectively inhibits differentiation into white

adipocytes but promotes brown-tissue and beige-cell adipogenesis, in good agreement with the natural rules of energy homeostasis [74].

Collectively, our data revealed that CT effectively induces brown adipogenesis in C3H10T1/2 cells accompanied by induction of mitochondrial biogenesis via AMPK and p38-MAPK signaling. Moreover, CT partially activates several beige-cell-specific markers and inhibits white-adipocyte specific genes. Because we did not assess the effect of CT on brown-fat adipogenesis *in vivo*, these effects need to be studied in the future. In conclusion, the findings of this study should point to new modalities for the treatment or prevention of obesity.

Author Contributions

NR, KMI and YSK designed the experiments. NR, KMI, DY, and MJ performed the experiments. NR, KMI, and YSK analyzed data and wrote the manuscript. Grant was supported by BTL and YSK.

Acknowledgments

This research was supported by Basic Science Research Program through the National Research Foundation of Korea (NRF) funded by the Ministry of Education (2015R1A6A1A03032522), and partially by a research fund of Soonchunhyang University.

References

[1] B. Cannon, J.A.N. Nedergaard, Brown adipose tissue: function and physiological significance, Physiol. Rev. 84 (2004) 277–359.

[2] X. Liu, M. Rossmeisl, J. McClaine, L.P. Kozak, Paradoxical resistance to diet-induced obesity in UCP1-deficient mice, J. Clin. Invest. 111 (2003) 399–407.

[3] K.A. Virtanen, W.D. van Marken Lichtenbelt, P. Nuutila, Brown adipose tissue functions in humans, Biochim. Biophys. Acta (BBA)-Molecular Cell Biol. Lipids. 1831 (2013) 1004–1008.

[4] M. Uldry, W. Yang, J. St-Pierre, J. Lin, P. Seale, B.M. Spiegelman, Complementary action of the PGC-1 coactivators in mitochondrial biogenesis and brown fat differentiation, Cell Metab. 3 (2006) 333–341.

[5] M. Saito, Y. Okamatsu-Ogura, M. Matsushita, K. Watanabe, T. Yoneshiro, J. Nio-Kobayashi, T. Iwanaga, M. Miyagawa, T. Kameya, K. Nakada, High incidence of metabolically active brown adipose tissue in healthy adult humans, Diabetes. 58 (2009) 1526–1531.

[6] J. Nedergaard, T. Bengtsson, B. Cannon, Unexpected evidence for active brown adipose tissue in adult humans, Am. J. Physiol. Metab. 293 (2007) E444–E452.

[7] A.M. Cypess, A.P. White, C. Vernochet, T.J. Schulz, R. Xue, C.A. Sass, T.L. Huang, C. Roberts-Toler, L.S. Weiner, C. Sze, Anatomical localization, gene expression profiling and functional characterization of adult human neck brown fat, Nat. Med. 19 (2013) 635–639.

[8] T. Shan, X. Liang, P. Bi, S. Kuang, Myostatin knockout drives browning of white adipose tissue through activating the AMPK-PGC1α-Fndc5 pathway in muscle, FASEB J. 27 (2013) 1981–1989.

[9] S. Kleiner, N. Douris, E.C. Fox, R.J. Mepani, F. Verdeguer, J. Wu, A. Kharitonenkov, J.S. Flier, E. Maratos-Flier, B.M. Spiegelman, FGF21 regulates PGC-1α and browning of white adipose tissues in adaptive thermogenesis, Genes Dev. 26 (2012) 271–281.

[10] O. Boss, S.R. Farmer, Recruitment of brown adipose tissue as a therapy for obesity-associated diseases, Front. Endocrynol. 3 (2013) 118–123.

[11] C. Hilton, F. Karpe, K.E. Pinnick, Role of developmental transcription factors in white, brown and beige adipose tissues, Biochim. Biophys. Acta - Mol. Cell Biol. Lipids. 1851 (2015) 686–696. doi:http://dx.doi.org/10.1016/j.bbalip.2015.02.003.

[12] C. Algire, D. Medrikova, S. Herzig, White and brown adipose stem cells: From signaling to clinical implications, Biochim. Biophys. Acta - Mol. Cell Biol. Lipids. 1831 (2013) 896–904. doi:http://dx.doi.org/10.1016/j.bbalip.2012.10.001.

[13] S.-W. Qian, Y. Tang, X. Li, Y. Liu, Y.-Y. Zhang, H.-Y. Huang, R.-D. Xue, H.-Y. Yu, L. Guo, H.-D. Gao, Y. Liu, X. Sun, Y.-M. Li, W.-P. Jia, Q.-Q. Tang, BMP4-mediated brown fat-like changes in white adipose tissue alter glucose and energy homeostasis, Proc. Natl. Acad. Sci. U. S. A. 110 (2013) E798–E807. doi:10.1073/pnas.1215236110.

[14] M.R. Boon, S.A.A. van den Berg, Y. Wang, J. van den Bossche, S. Karkampouna, M. Bauwens, M. De Saint-Hubert, G. van der Horst, S. Vukicevic, M.P.J. de Winther, L.M. Havekes, J.W. Jukema, J.T. Tamsma, G. van der Pluijm, K.W. van Dijk, P.C.N. Rensen, BMP7 activates brown adipose tissue and reduces diet-induced obesity only at subthermoneutrality., PLoS One. 8 (2013) e74083. doi:10.1371/journal.pone.0074083.

[15] S. Modica, C. Wolfrum, Bone morphogenic proteins signaling in adipogenesis and energy homeostasis, Biochim. Biophys. Acta - Mol. Cell Biol. Lipids. 1831 (2013) 915–923. doi:http://dx.doi.org/10.1016/j.bbalip.2013.01.010.

[16] M. Elsen, S. Raschke, N. Tennagels, U. Schwahn, T. Jelenik, M. Roden, T. Romacho,

J. Eckel, BMP4 and BMP7 induce the white-to-brown transition of primary human adipose stem cells, Am. J. Physiol. Physiol. 306 (2014) C431–C440.

[17] R. Xue, Y. Wan, S. Zhang, Q. Zhang, H. Ye, Y. Li, Role of bone morphogenetic protein 4 in the differentiation of brown fat-like adipocytes, Am. J. Physiol. Metab. 306 (2014) E363–E372.

[18] L. Sturla, E. Mannino, S. Scarfì, S. Bruzzone, M. Magnone, G. Sociali, V. Booz, L. Guida, T. Vigliarolo, C. Fresia, L. Emionite, A. Buschiazzo, C. Marini, G. Sambuceti, A. De Flora, E. Zocchi, Abscisic acid enhances glucose disposal and induces brown fat activity in adipocytes in vitro and in vivo, Biochim. Biophys. Acta - Mol. Cell Biol. Lipids. 1862 (2017) 131–144. doi:http://dx.doi.org/10.1016/j.bbalip.2016.11.005.

[19] J. Lone, J.H. Choi, S.W. Kim, J.W. Yun, Curcumin induces brown fat-like phenotype in 3T3-L1 and primary white adipocytes, J. Nutr. Biochem. 27 (2016) 193–202. doi:http://dx.doi.org/10.1016/j.jnutbio.2015.09.006.

[20] S. Wang, X. Liang, Q. Yang, X. Fu, C.J. Rogers, M. Zhu, B.D. Rodgers, Q. Jiang, M. V Dodson, M. Du, Resveratrol induces brown-like adipocyte formation in white fat through activation of AMP-activated protein kinase (AMPK) alpha1., Int. J. Obes. (Lond). 39 (2015) 967–976. doi:10.1038/ijo.2015.23.

[21] H.Q. Zhang, S.Y. Chen, A.S. Wang, A.J. Yao, J.F. Fu, J.S. Zhao, F. Chen, Z.Q. Zou, X.H. Zhang, Y.J. Shan, Sulforaphane induces adipocyte browning and promotes glucose and lipid utilization, Mol. Nutr. Food Res. 60 (2016) 2185–2197.

[22] N.-J. Song, S. Choi, P. Rajbhandari, S.-H. Chang, S. Kim, L. Vergnes, S.-M. Kwon, J.-H. Yoon, S. Lee, J.-M. Ku, Prdm4 induction by the small molecule butein promotes white adipose tissue browning, Nat. Chem. Biol. 12 (2016) 479–481.

[23] E.J. Kim, S.-N. Jung, K.H. Son, S.R. Kim, T.Y. Ha, M.G. Park, I.G. Jo, J.G. Park, W.

Choe, S.-S. Kim, Antidiabetes and antiobesity effect of cryptotanshinone via activation of AMP-activated protein kinase, Mol. Pharmacol. 72 (2007) 62–72.

[24] L. Zhou, Z. Zuo, M.S.S. Chow, Danshen: an overview of its chemistry, pharmacology, pharmacokinetics, and clinical use, J. Clin. Pharmacol. 45 (2005) 1345–1359.

[25] N. Rahman, M. Jeon, H.-Y. Song, Y.-S. Kim, Cryptotanshinone, a compound of Salvia miltiorrhiza inhibits pre-adipocytes differentiation by regulation of adipogenesis-related genes expression via STAT3 signaling., Phytomedicine. 23 (2016) 58–67. doi:10.1016/j.phymed.2015.12.004.

[26] N. Rahman, M. Jeon, Y.-S. Kim, Delphinidin, a major anthocyanin, inhibits 3T3-L1 pre-adipocyte differentiation through activation of Wnt/beta-catenin signaling., Biofactors. 42 (2016) 49–59. doi:10.1002/biof.1251.

[27] Y.J. Koh, B.-H. Park, J.-H. Park, J. Han, I.-K. Lee, J.W. Park, G.Y. Koh, Activation of PPAR[gamma] induces profound multilocularization of adipocytes in adult mouse white adipose tissues, Exp Mol Med. 41 (2009) 880–895. http://dx.doi.org/10.3858/emm.2009.41.12.094.

[28] L. Schild, F. Dombrowski, U. Lendeckel, C. Schulz, A. Gardemann, G. Keilhoff, Impairment of endothelial nitric oxide synthase causes abnormal fat and glycogen deposition in liver., Biochim. Biophys. Acta. 1782 (2008) 180–187. doi:10.1016/j.bbadis.2007.12.007.

[29] J.M.A. de Jong, O. Larsson, B. Cannon, J. Nedergaard, A stringent validation of mouse adipose tissue identity markers, Am. J. Physiol. Metab. 308 (2015) E1085–E1105.

[30] W. Cao, A. V Medvedev, K.W. Daniel, S. Collins, β-adrenergic activation of p38 MAP kinase in adipocytes cAMP induction of the uncoupling protein 1 (UCP1) gene

requires p38 map kinase, J. Biol. Chem. 276 (2001) 27077–27082.

[31] N.L. Price, C. Fernández-Hernando, miRNA regulation of white and brown adipose tissue differentiation and function, Biochim. Biophys. Acta (BBA)-Molecular Cell Biol. Lipids. 1861 (2016) 2104–2110.

[32] P.J. Fernandez-Marcos, J. Auwerx, Regulation of PGC-1α, a nodal regulator of mitochondrial biogenesis, Am. J. Clin. Nutr. 93 (2011) 884S–890S.

[33] L. Wilson-Fritch, A. Burkart, G. Bell, K. Mendelson, J. Leszyk, S. Nicoloro, M. Czech, S. Corvera, Mitochondrial biogenesis and remodeling during adipogenesis and in response to the insulin sensitizer rosiglitazone, Mol. Cell. Biol. 23 (2003) 1085–1094.

[34] B.L. Tang, Sirt1 and the Mitochondria, Mol. Cells. 39 (2016) 87.

[35] Y.-H. Tseng, E. Kokkotou, T.J. Schulz, T.L. Huang, J.N. Winnay, C.M. Taniguchi, T.T. Tran, R. Suzuki, D.O. Espinoza, Y. Yamamoto, M.J. Ahrens, A.T. Dudley, A.W. Norris, R.N. Kulkarni, C.R. Kahn, New role of bone morphogenetic protein 7 in brown adipogenesis and energy expenditure., Nature. 454 (2008) 1000–1004. doi:10.1038/nature07221.

[36] S. Rajakumari, J. Wu, J. Ishibashi, H.-W. Lim, A.-H. Giang, K.-J. Won, R.R. Reed, P. Seale, EBF2 determines and maintains brown adipocyte identity, Cell Metab. 17 (2013) 562–574.

[37] M.A. Jimenez, P. Åkerblad, M. Sigvardsson, E.D. Rosen, Critical role for Ebf1 and Ebf2 in the adipogenic transcriptional cascade, Mol. Cell. Biol. 27 (2007) 743–757.

[38] X. Liu, R.R. Chhipa, I. Nakano, B. Dasgupta, The AMPK inhibitor compound C is a potent AMPK-independent antiglioma agent., Mol. Cancer Ther. 13 (2014) 596–605. doi:10.1158/1535-7163.MCT-13-0579.

[39] M. Barancik, V. Bohacova, J. Kvackajova, S. Hudecova, O. Krizanova, A. Breier, SB203580, a specific inhibitor of p38-MAPK pathway, is a new reversal agent of P-glycoprotein-mediated multidrug resistance., Eur. J. Pharm. Sci. 14 (2001) 29–36.

[40] K.A. Virtanen, M.E. Lidell, J. Orava, M. Heglind, R. Westergren, T. Niemi, M. Taittonen, J. Laine, N.-J. Savisto, S. Enerbäck, Functional brown adipose tissue in healthy adults, N. Engl. J. Med. 360 (2009) 1518–1525.

[41] W.D. van Marken Lichtenbelt, J.W. Vanhommerig, N.M. Smulders, J.M. Drossaerts, G.J. Kemerink, N.D. Bouvy, P. Schrauwen, G.J.J. Teule, Cold-activated brown adipose tissue in healthy men, N. Engl. J. Med. 360 (2009) 1500–1508.

[42] P. Valet, G. Tavernier, I. Castan-Laurell, J.S. Saulnier-Blache, D. Langin, Understanding adipose tissue development from transgenic animal models, J. Lipid Res. 43 (2002) 835–860.

[43] P. Polak, N. Cybulski, J.N. Feige, J. Auwerx, M.A. Rüegg, M.N. Hall, Adipose-specific knockout of raptor results in lean mice with enhanced mitochondrial respiration, Cell Metab. 8 (2008) 399–410.

[44] H. Ohno, K. Shinoda, B.M. Spiegelman, S. Kajimura, PPARγ agonists induce a white-to-brown fat conversion through stabilization of PRDM16 protein, Cell Metab. 15 (2012) 395–404.

[45] P. Seale, Transcriptional regulatory circuits controlling brown fat development and activation, Diabetes. 64 (2015) 2369–2375.

[46] T.J. Schulz, P. Huang, T.L. Huang, R. Xue, L.E. McDougall, K.L. Townsend, A.M. Cypess, Y. Mishina, E. Gussoni, Y.-H. Tseng, Brown-fat paucity due to impaired BMP signalling induces compensatory browning of white fat, Nature. 495 (2013) 379–383.

[47] H. Zhang, M. Guan, K.L. Townsend, T.L. Huang, D. An, X. Yan, R. Xue, T.J. Schulz,

J. Winnay, M. Mori, M.F. Hirshman, K. Kristiansen, J.S. Tsang, A.P. White, A.M. Cypess, L.J. Goodyear, Y.-H. Tseng, MicroRNA-455 regulates brown adipogenesis via a novel HIF1an-AMPK-PGC1alpha signaling network., EMBO Rep. 16 (2015) 1378–1393. doi:10.15252/embr.201540837.

[48] D.G. Hardie, AMPK: a key regulator of energy balance in the single cell and the whole organism, Int J Obes. 32 (n.d.) S7–S12. http://dx.doi.org/10.1038/ijo.2008.116.

[49] Y. Zhang, R. Li, Y. Meng, S. Li, W. Donelan, Y. Zhao, L. Qi, M. Zhang, X. Wang, T. Cui, Irisin stimulates browning of white adipocytes through mitogen-activated protein kinase p38 MAP kinase and ERK MAP kinase signaling, Diabetes. 63 (2014) 514–525.

[50] H. Huang, T.-J. Song, X. Li, L. Hu, Q. He, M. Liu, M.D. Lane, Q.-Q. Tang, BMP signaling pathway is required for commitment of C3H10T1/2 pluripotent stem cells to the adipocyte lineage., Proc. Natl. Acad. Sci. U. S. A. 106 (2009) 12670–12675. doi:10.1073/pnas.0906266106.

[51] S.G. Rane, H. Yadav, TGF-β/Smad3 signaling regulates brown adipocyte induction in white adipose tissue, Front. Endocrinol. (Lausanne). 3 (2012) 35.

[52] P. Seale, S. Kajimura, W. Yang, S. Chin, L.M. Rohas, M. Uldry, G. Tavernier, D. Langin, B.M. Spiegelman, Transcriptional Control of Brown Fat Determination by PRDM16, Cell Metab. 6 (2007) 38–54. doi:10.1016/j.cmet.2007.06.001.

[53] P. Puigserver, Z. Wu, C.W. Park, R. Graves, M. Wright, B.M. Spiegelman, A cold-inducible coactivator of nuclear receptors linked to adaptive thermogenesis, Cell. 92 (1998) 829–839.

[54] T.L. Rachid, A. Penna-de-Carvalho, I. Bringhenti, M.B. Aguila, C.A. Mandarim-de-Lacerda, V. Souza-Mello, Fenofibrate (PPARalpha agonist) induces beige cell

formation in subcutaneous white adipose tissue from diet-induced male obese mice, Mol. Cell. Endocrinol. 402 (2015) 86–94.

[55] Y. Kontani, Y. Wang, K. Kimura, K. Inokuma, M. Saito, T. Suzuki- Miura, Z. Wang, Y. Sato, N. Mori, H. Yamashita, UCP1 deficiency increases susceptibility to diet- induced obesity with age, Aging Cell. 4 (2005) 147–155.

[56] H.M. Feldmann, V. Golozoubova, B. Cannon, J. Nedergaard, UCP1 ablation induces obesity and abolishes diet-induced thermogenesis in mice exempt from thermal stress by living at thermoneutrality, Cell Metab. 9 (2009) 203–209.

[57] S. Kajimura, P. Seale, B.M. Spiegelman, Transcriptional control of brown fat development, Cell Metab. 11 (2010) 257–262.

[58] T. Inagaki, J. Sakai, S. Kajimura, Transcriptional and epigenetic control of brown and beige adipose cell fate and function, Nat. Rev. Mol. Cell Biol. 17 (2016) 480–495.

[59] M. del Mar Gonzalez-Barroso, C. Pecqueur, C. Gelly, D. Sanchis, M.C. Alves-Guerra, F. Bouillaud, D. Ricquier, A.M. Cassard-Doulcier, Transcriptional activation of the human ucp1 gene in a rodent cell line. Synergism of retinoids, isoproterenol, and thiazolidinedione is mediated by a multipartite response element., J. Biol. Chem. 275 (2000) 31722–31732. doi:10.1074/jbc.M001678200.

[60] I.B. Sears, M.A. MacGinnitie, L.G. Kovacs, R.A. Graves, Differentiation-dependent expression of the brown adipocyte uncoupling protein gene: regulation by peroxisome proliferator-activated receptor gamma., Mol. Cell. Biol. 16 (1996) 3410–3419. http://www.ncbi.nlm.nih.gov/pmc/articles/PMC231335/.

[61] R. Rabelo, A. Schifman, A. Rubio, X. Sheng, J.E. Silva, Delineation of thyroid hormone-responsive sequences within a critical enhancer in the rat uncoupling protein gene., Endocrinology. 136 (1995) 1003–1013. doi:10.1210/endo.136.3.7867554.

[62] A.M. Cassard-Doulcier, M. Larose, J.C. Matamala, O. Champigny, F. Bouillaud, D. Ricquier, In vitro interactions between nuclear proteins and uncoupling protein gene promoter reveal several putative transactivating factors including Ets1, retinoid X receptor, thyroid hormone receptor, and a CACCC box-binding protein., J. Biol. Chem. 269 (1994) 24335–24342.

[63] U.C. Kozak, J. Kopecky, J. Teisinger, S. Enerbäck, B. Boyer, L.P. Kozak, An upstream enhancer regulating brown-fat-specific expression of the mitochondrial uncoupling protein gene., Mol. Cell. Biol. 14 (1994) 59–67. http://www.ncbi.nlm.nih.gov/pmc/articles/PMC358356/.

[64] B.B. Boyer, L.P. Kozak, The mitochondrial uncoupling protein gene in brown fat: correlation between DNase I hypersensitivity and expression in transgenic mice., Mol. Cell. Biol. 11 (1991) 4147–4156.

[65] V. Calabrese, G. Scapagnini, A.M. Giuffrida Stella, T.E. Bates, J.B. Clark, Mitochondrial involvement in brain function and dysfunction: relevance to aging, neurodegenerative disorders and longevity., Neurochem. Res. 26 (2001) 739–764.

[66] M.A. Tarnopolsky, S. Raha, Mitochondrial myopathies: diagnosis, exercise intolerance, and treatment options., Med. Sci. Sports Exerc. 37 (2005) 2086–2093.

[67] D.C. Wallace, A mitochondrial paradigm of metabolic and degenerative diseases, aging, and cancer: a dawn for evolutionary medicine., Annu. Rev. Genet. 39 (2005) 359–407. doi:10.1146/annurev.genet.39.110304.095751.

[68] S.D. Martin, S.L. McGee, The role of mitochondria in the aetiology of insulin resistance and type 2 diabetes, Biochim. Biophys. Acta - Gen. Subj. 1840 (2014) 1303–1312. doi:http://dx.doi.org/10.1016/j.bbagen.2013.09.019.

[69] J. Lin, C. Handschin, B.M. Spiegelman, Metabolic control through the PGC-1 family

of transcription coactivators, Cell Metab. 1 (2005) 361–370.

[70] C.-L. Zhang, H. Feng, L. Li, J.-Y. Wang, D. Wu, Y.-T. Hao, Z. Wang, Y. Zhang, L.-L. Wu, Globular CTRP3 promotes mitochondrial biogenesis in cardiomyocytes through AMPK/PGC-1α pathway, Biochim. Biophys. Acta - Gen. Subj. 1861 (2017) 3085–3094. doi:http://dx.doi.org/10.1016/j.bbagen.2016.10.022.

[71] M. Fernández-Galilea, P. Pérez-Matute, P.L. Prieto-Hontoria, M. Houssier, M.A. Burrell, D. Langin, J.A. Martínez, M.J. Moreno-Aliaga, α-Lipoic acid treatment increases mitochondrial biogenesis and promotes beige adipose features in subcutaneous adipocytes from overweight/obese subjects, Biochim. Biophys. Acta - Mol. Cell Biol. Lipids. 1851 (2015) 273–281. doi:http://dx.doi.org/10.1016/j.bbalip.2014.12.013.

[72] M. Correia, T. Perestrelo, A.S. Rodrigues, M.F. Ribeiro, S.L. Pereira, M.I. Sousa, J. Ramalho-Santos, Sirtuins in metabolism, stemness and differentiation, Biochim. Biophys. Acta - Gen. Subj. 1861 (2017) 3444–3455. doi:http://dx.doi.org/10.1016/j.bbagen.2016.09.008.

[73] M.R. de Oliveira, S.F. Nabavi, A. Manayi, M. Daglia, Z. Hajheydari, S.M. Nabavi, Resveratrol and the mitochondria: from triggering the intrinsic apoptotic pathway to inducing mitochondrial biogenesis, a mechanistic view, Biochim. Biophys. Acta (BBA)-General Subj. 1860 (2016) 727–745.

[74] E.D. Rosen, B.M. Spiegelman, Adipocytes as regulators of energy balance and glucose homeostasis, Nature. 444 (2006) 847–853.

Figure legends

Fig. 1. Effects of CT on the commitment of C3H10T1/2 mesenchymal stem cells to the adipocyte lineage. C3H10T1/2 cells were seeded at low confluence and were incubated with a growth medium or growth medium supplemented or not supplemented with 50 μM BMP4 before exposure to adipogenic hormonal stimuli (MDI). Then, the cells were treated with MDI supplemented or not supplemented with 8 μM CT. ORO staining, preparation of RNA and protein was performed at day 8. (A) Treatment course, (B) ORO staining images of treatment groups with BMP4 pretreatment. (C) ORO staining images of treatment groups without BMP4 pretreatment of C3H10T1/2 and 3T3-L1 cells (PA refers to preadipocytes).

Fig. 2. Effects of CT on the expression of BAT-specific markers in C3H10T1/2 cells. These cells were seeded at low confluence and were incubated with the growth medium or growth medium supplemented with 50 nM BMP4 until 2 days post confluence. Next, the cells were induced to differentiate by adding adipogenic hormonal stimuli (into the culture medium) with or without 8 μM CT. Total RNA samples were collected on day 8 and subjected to qRT-PCR for the analysis of (A) Expression of BAT-specific and Beige-cell-specific genes. (B) Expression of WAT-specific genes. (C) Expression of Myogenesis and Condrogenesis-specific genes. Gene expression data were normalized to that of *Gapdh*, and the results were expressed as relative fold induction. Data are presented as mean ± SD of no less than two independent experiments (*P < 0.05, **P < 0.01, ***P < .001).

Fig. 3. Effects of CT on differentiation into brown adipocytes. (A) A *Ucp1* reporter gene assay in both 3T3-L1 and C3H10T1/2 cells. Results were normalized to the *Renilla* luciferase control and were expressed as a fold change relative to the control (MDI). (B) C3H10T1/2 and iWAT cells were grown and treated as described in Materials and methods section 2.2,

then protein levels were analyzed by western blotting. Quantification of western blot images is shown beneath the data. (C) C3H10T1/2 cells were treated with rosiglitazone or CT under MDI conditions, then stained with Bodipy and DAPI; the right panel represents an inset.

Fig. 4. Effects of CT on mitochondrial biogenesis. C3H10T1/2 cells were grown and treated as described above. (A) Total RNA samples were collected on day 8 and subjected to qRT-PCR for the analysis of expression levels of mitochondrial-biogenesis-related genes. Gene expression was normalized to *Gapdh*, and the results were expressed as relative fold induction. Data are presented as mean ± SD of at least three independent experiments (*P < 0.05, **P < 0.01). (B) Mitochondrial mass was evaluated by Mito-tracker (Red) and Ucp1 (Green) staining on day 8. (C) Protein expression of Sirt1 in C3H10T1/2 cells treated with rosiglitazone (1 μM), BMP7 (10 ng/ml), or CT (8 μM) along with MDI. (D) The proportion of mitochondrial DNA. (E) Quantification of Mitotracker and Ucp1 staining images was carried out by ImageJ software. Data are shown as mean ± SD of at least two independent experiments (*P < 0.05, **P < 0.01, ***P < 0.001).

Fig. 5. Effects of CT on expression of commitment-related genes and AMPK and p38-MAPK signaling in C3H10T1/2 cells. (A) Total RNA samples were collected on day 2 and subjected to qRT-PCR for the analysis of commitment by means of expression levels of the brown-adipocyte-related genes. Gene expression was normalized to *Gapdh*, and the results were expressed as a relative fold induction. Data are presented as mean ± SD of at least three independent experiments (*P < 0.05, **P < 0.01 and $^{\#}$P < 0.05, $^{\#\#}$P < 0.01 refers to significant differences with preadipocyte (PA) and MDI control groups respectively). (B) C3H10T1/2 cells were grown to full confluence, then were serum starved for 4 hr and treated with 8 μM CT for the indicated periods of time. Then, the amount of p-38, P-p-38, AMPKα, p-AMPKα

was measured by western blotting. Two sets of C3H10T1/2 cells after 4-hr serum starvation were incubated with 10 μM dorsomorphin (Dorso) and 50 μM SB203580 or in combination for 2 hr and then for 30 min with or without 8 μM CT as indicated. Then, 1 set of cells was used to extract total protein, which was collected and subjected to western blot analysis (C). Another set of cells was kept for 48 hr after media change and total RNA was collected and qRT-PCR analysis was performed (D).

Fig. 6. Effects of p38-MAPKα gene silencing on the expression of commitment-related genes and corresponding signaling in C3H10T1/2 mesenchymal stem cells. Gene silencing study of p38-MAPKα and collection of RNA and protein were performed as described in Methods and Materials section. (A) WB blot analyses were performed using p-38, Smad1, p-Smad1/5, p-AMPKα and AMPKα. β-actin was used as internal control. (B) Total RNA samples were collected on day 2 and subjected to qRT-PCR for the analysis of commitment by means of expression levels of the brown-adipocyte-related genes. Gene expression was normalized to *Gapdh*, and the results were expressed as a relative fold induction. Data are presented as mean ± SD of at least three independent experiments (*$P < 0.05$, **$P < 0.01$ and ***$P < 0.001$ refers to significant differences with MDI control groups.

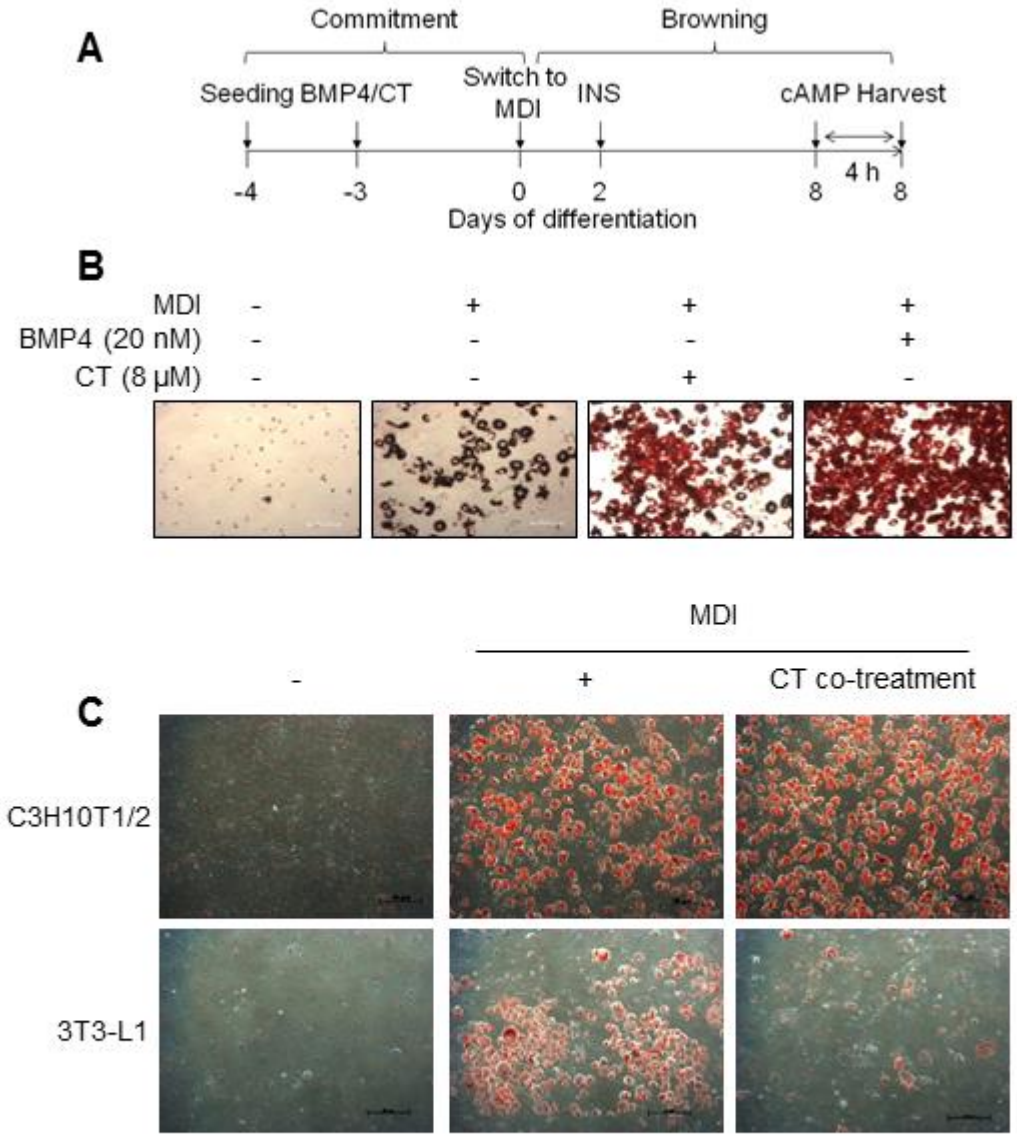

Fig. 1

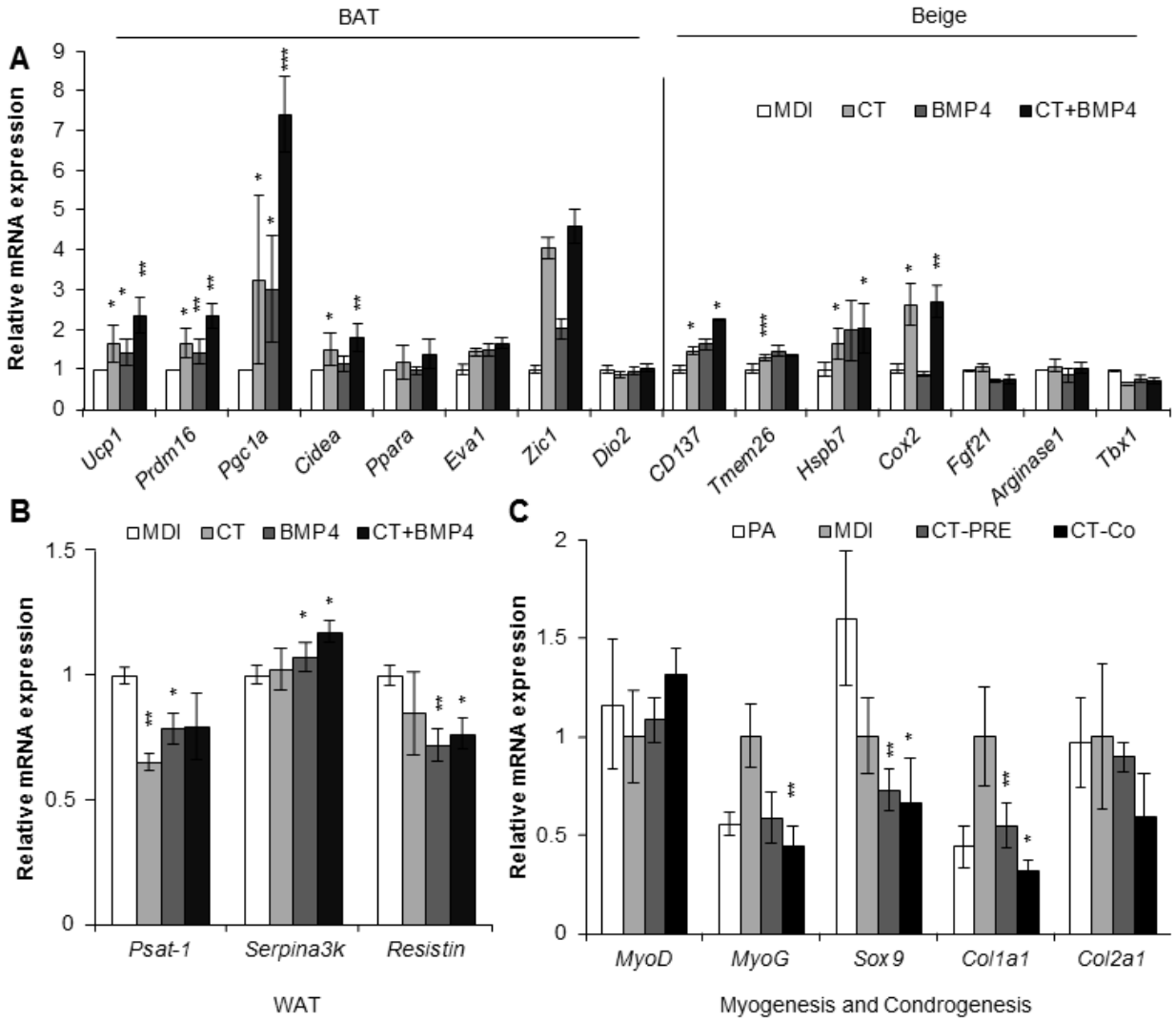
BAT
Beige
A
Relative mRNA expression
MDI
CT
BMP4
CT+BMP4
Ucp1
Prdm16
Pgc1a
Cidea
Ppara
Eva1
Zic1
Dio2
CD137
Tmem26
Hspb7
Cox2
Fgf21
Arginase1
Tbx1
B
Psat-1
Serpina3k
Resistin
WAT
C
PA
CT-PRE
CT-Co
MyoD
MyoG
Sox9
Col1a1
Col2a1
Myogenesis and Condrogenesis

Fig. 2

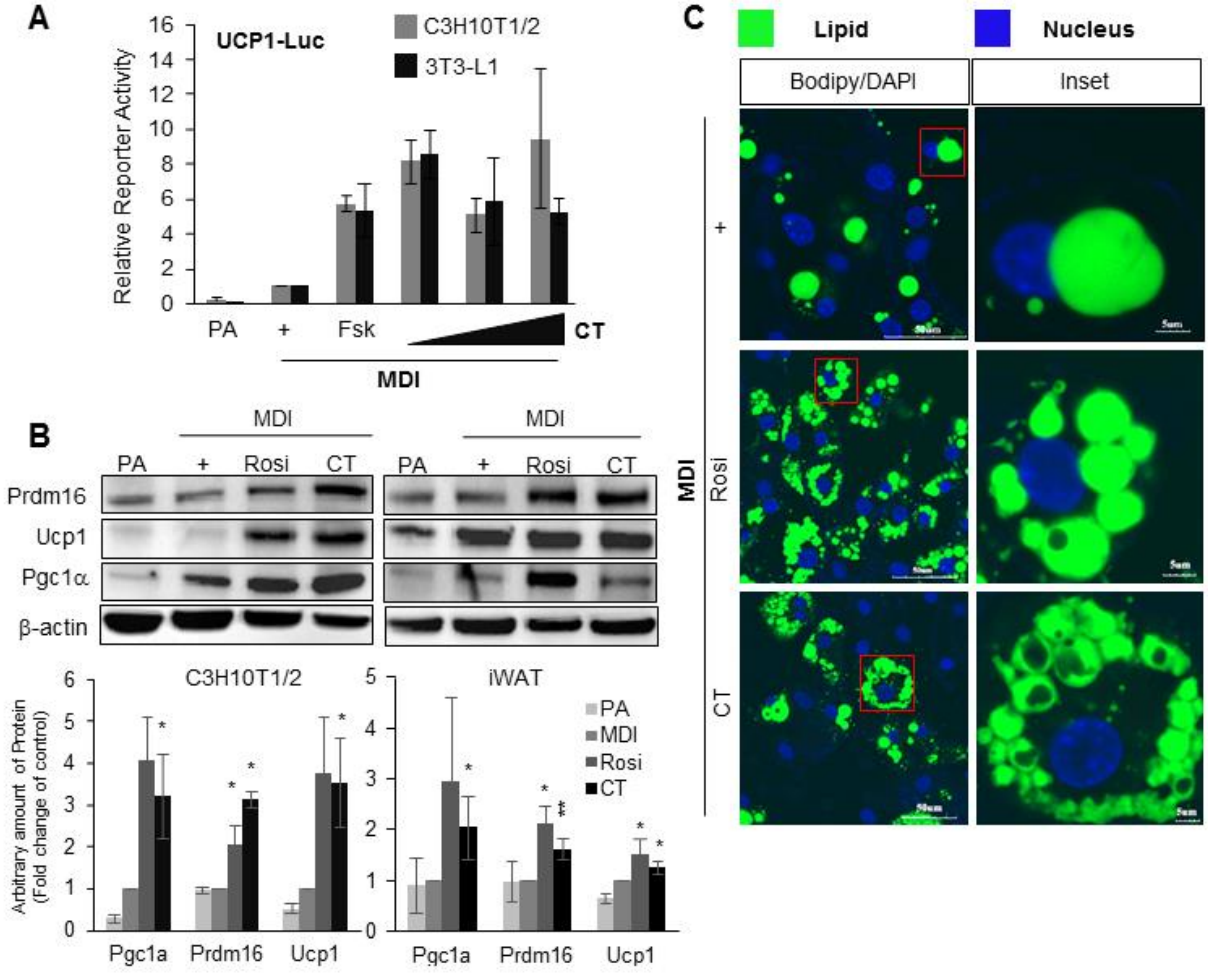

Fig. 3

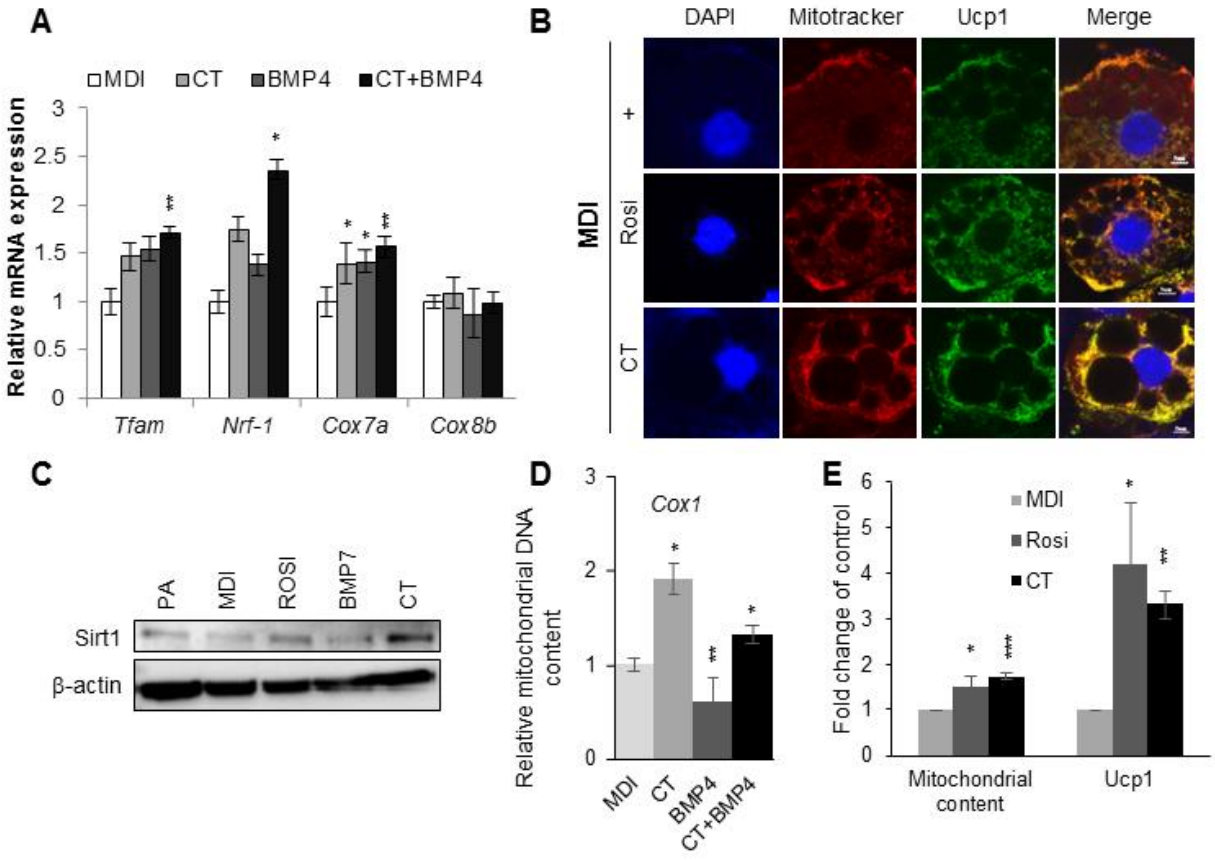

Fig. 4

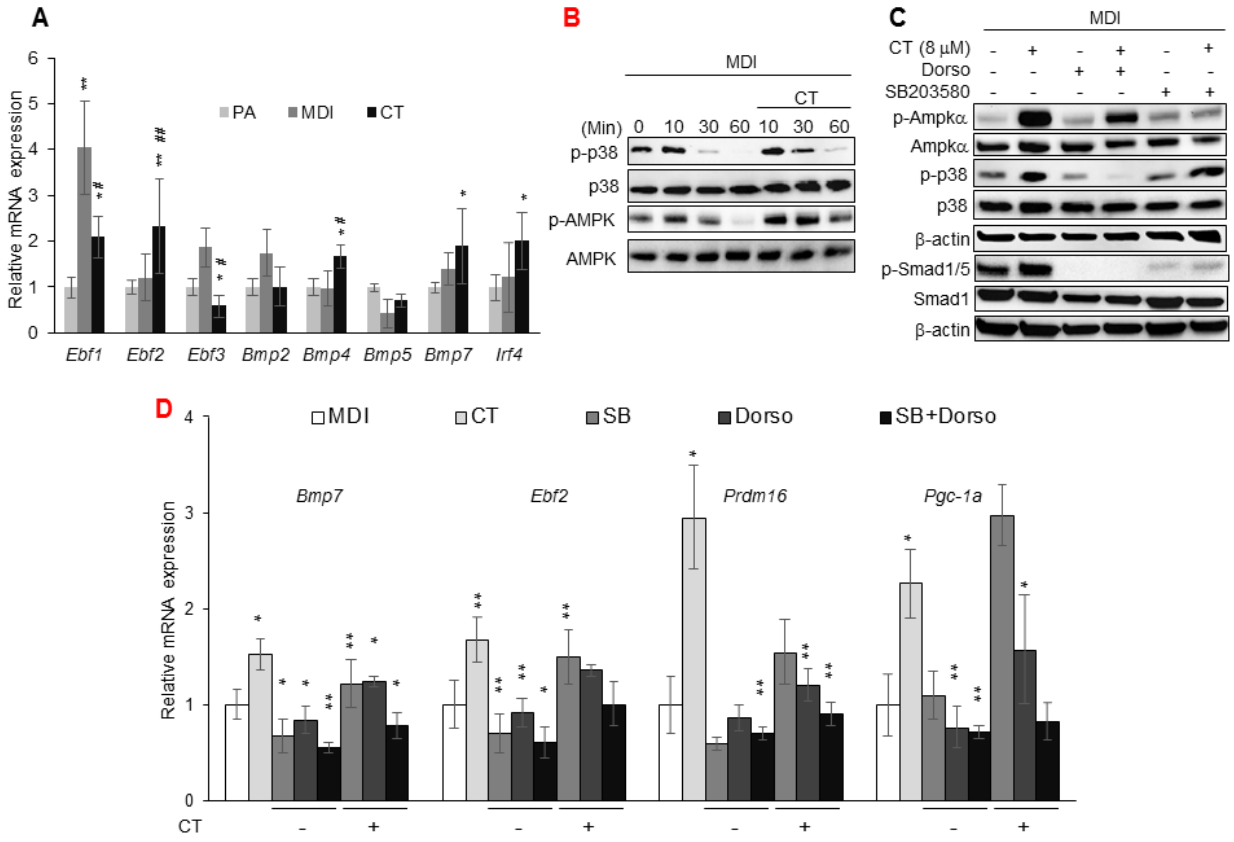

Fig. 5

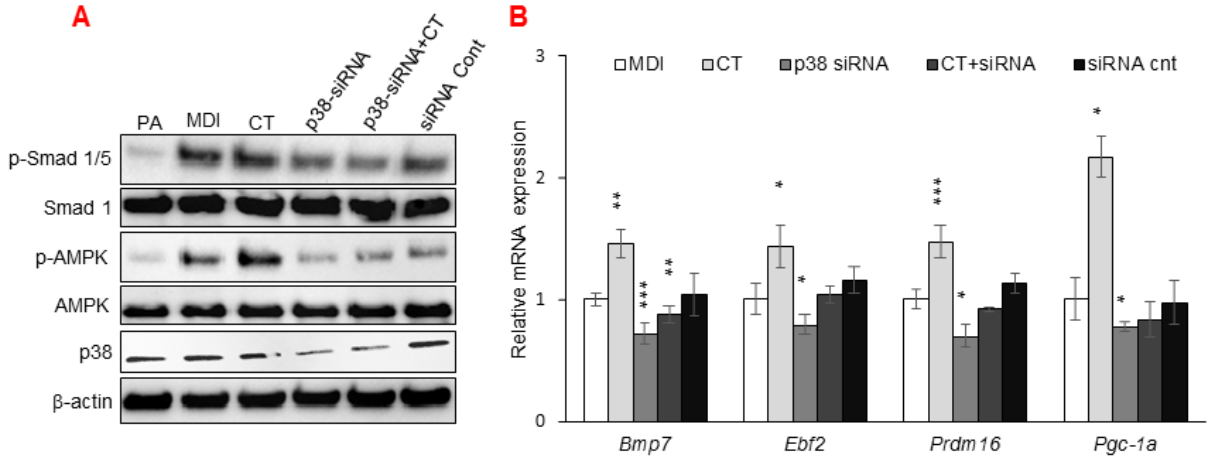

Fig. 6

Table 1. Primer Sequences used for q-RT-PCR of mouse genes in this study

Primer	Forward	Reverse
Bmp2	GGGACCCGCTGTCTTCTAGT	TCAACTCAAATTCGCTGAGG
Bmp4	GACTTCGAGGCGACACTTCT	GCCGGTAAAGATCCCTCATG
Bmp5	TTACTTAGGGGTATTGTGGG	CCGTCTCTCATGGTTCCGTA
Bmp7	ACGGACAGGGCTTCTCCTAC	ATGGTGGTATCGAGGGTGGA
Cidea	TGCTCTTCTGTATCGCCCAGT	GCCGTGTTAAGGAATCTGCTG
Cox1	TCTACTATTCGGAGCCTGAG	CTACTGATGCTCCTGCATGG
Cox7a	CAGCGTCATGGTCAGTCTGT	AGAAAACCGTGTGGCAGAGA
Cox8b	GAACCATGAAGCCAACGACT	CGCAAGTTCACAGTCGTTCC
Dio2	CAGTGTGGTGCACGTCTCCAATC	TGAACCCCCGTTGACCACCAG
Ebf1	AAGGATGGACGACGGGAGGCG	GGGATGTGCCGAGGAGGTGTCT
Ebf2	GCTGCGGGAACCGGAACGAGA	ACACGACCTGGAACCGCCTCA
Ebf3	CGAAAGGACCGCTTTTGTGG	AGTGAATGCCGTTGTTGGTTT
Gapdh	GACATGCCGCCTGGAGAAAC	AGCCCAGGATGCCCTTTAGT
Hspb7	GAGCATGTTTTCAGACGACTTTG	CCGAGGGTCTTCATGTTTCCTT
Irf4	GCAGCTCACTTTGGATGACA	CCAAACGTCACAGGACATTG
MyoD	CGCCACTCCGGGACATAG	GAAGTCGTCTGCTGTCTCAAAGG
MyoG	AGCGCAGGCTCAAGAAAGTGAATG	CTGTAGGCGCTCAATGTACTGGAT
Sox9	CGG AGG AAG TCG GTG AAG A	GTC GGT TTT GGG AGT GGT G
Col1a1	GCATGGCCAAGAAGACATCC	CCTCGGGTTTCCACGTCTC
Col2a1	CCACACCAAATTCCTGTTCA	ACTGGTAAGTGGGGCAAGAC
Aginase1	TGGCTTGCGAGACGTAGAC	GCTCAGGTGAATCGGCCTTTT
CD137	CGTGCAGAACTCCTGTGATAAC	GTCCACCTATGCTGGAGAAGG
Cox2	GACTGGGCCATGGAGTGG	CACCTCTCCACCAATGACC
Eva1	CCACTTCTCCTGAGTTTACAGC	GCATTTTAACCGAACATCTGTCC
Fgf21	AGATCAGGGAGGATGGAACA	TCAAAGTGAGGCGATCCATA
Tbx1	GGCAGGCAGACGAATGTTC	TTGTCATCTACGGGCACAAAG
Tmem26	ACCCTGTCATCCCACAGAG	TGTTTGGTGGAGTCCTAAGGTC
Nrf1	CAACAGGGAAGAAACGGAAA	GCACCACATTCTCCAAAGGT
p0	GCACTTTCGCTTTCTGGAGGGTGT	TGACTTGGTTGCTTTGGCGGGATT
Pgc-1α	ACAGCTTTCTGGGTGGATT	TGAGGACCGCTAGCAAGTTT
Pparα	GCGTACGGCAATGGCTTTAT	GAACGGCTTCAGGTTCTT
Prdm16	CAGCACGGTGAAGCCATTC	GCGTGCATCCGCTTGTG
Psat1	TACCGCCTTGTCAAGAAACC	AGTGGAGCGCCAGAATAGAA
Resistin	TGC CAG TGT GCA AGG ATA GAC T	CGC TCA CTT CCC CGA CAT
Serpina3k	GGCTGAAGGCAAAGTCAGTGT	TGGAATCTGTCCTGCTGTCCT
Tfam	GTCCATAGGCACCGTATTGC	CCCATGCTGGAAAAACACTT
Ucp1	GGCATTCAGAGGCAAATCAGCT	CAATGAACACTGCCACACCTC

Zic1	CTGTTGTGGGAGACACGATG	CTGTTGTGGGAGACACGATG

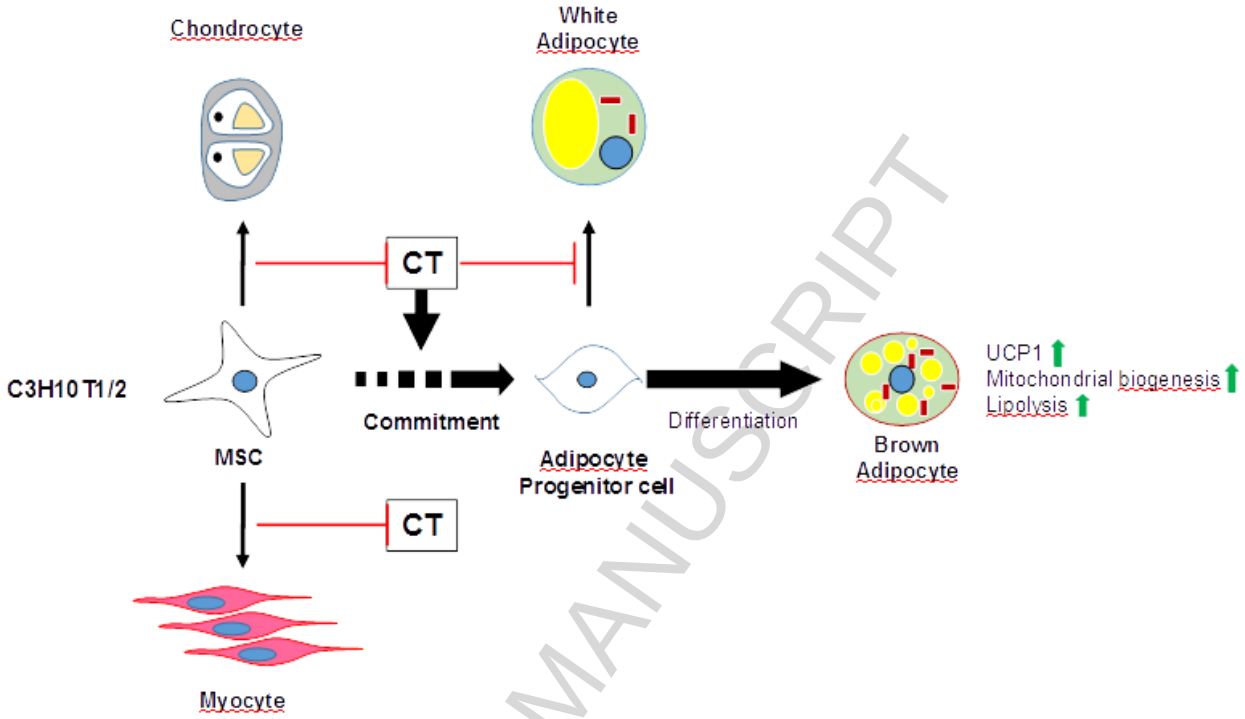

Graphical abstract

Highlights

- Treatment of CT promotes expression of brown and beige-specific markers.
- CT activates the expression of Ucp1 gene in C3H10T1/2 mesenchymal stem cells.
- CT induces mitochondrial biogenesis in C3H10T1/2 mesenchymal stem cells.
- Both p38-MAPK and AMPK signaling is important in CT-mediated brown adipocyte differentiation from C3H10T1/2 mesenchymal stem cells.